Journal of Atmospheric and Solar-Terrestrial Physics 71 (2009) 636–643

Contents lists available at ScienceDirect

Journal of Atmospheric and Solar-Terrestrial Physics

journal homepage: www.elsevier.com/locate/jastp

Meteor-head echo observations using an antenna compression approach with the 450 MHz Poker Flat Incoherent Scatter Radar

Jorge L. Chau [a,*], Freddy R. Galindo [a], Craig J. Heinselman [b], Michael J. Nicolls [b]

[a] Radio Observatorio de Jicamarca, Instituto Geofísico del Perú, Lima, Peru
[b] Center for Geospace Studies, SRI International, Menlo Park, CA, USA

ARTICLE INFO

Article history:
Accepted 21 August 2008
Available online 6 September 2008

Keywords:
Meteors
Meteoroids
Ionosphere
Radar

ABSTRACT

In this work we present a novel use of the Poker Flat Incoherent Scatter Radar (PFISR) to study meteor-head echoes with wide (W) beams. Until now, most of the meteor-head echo studies have been performed with High-Power Large-Aperture Radars (HPLARs) using very narrow (N) beams. At PFISR we have implemented an antenna compression approach using a defocusing scheme, similar to Chirp (linear frequency modulation) in pulse compression. The resulting effective beam is ~3 times wider than the narrowest PFISR beam. Using the signal-to-noise ratio (SNR) as a proxy measurement of cross-section, from the combined W and N beam experiments, our main results are: (1) observed meteors in the W beam are approximately half the number of meteors observed in the N beam, (2) we detected 10 times more large cross-section (strong) meteors (>15 dB if they were measured by the N mainlobe) than using only the N beam, and (3) more than 15% of the total N meteors were observed in the N sidelobes, therefore being at least 20 dB stronger if they were observed in the N mainlobe. Our results are summarized in a corrected distribution of relative meteor cross-sections as if all of them were observed with the N mainlobe, namely correcting their SNR values depending on where in the beam they were detected (sidelobes or mainlobe). In addition, we show a qualitative meteor cross-section distribution that one can obtain combining W and N beams. The resulting distribution is incomplete, since the W beam is not sensitive enough to detect the very small (weak) meteors, but could provide new information about the large cross-section events.

1. Introduction

Since mid 1990s extensive meteor-head echo observations have been performed with different High-Power Large-Aperture Radars (HPLARs) (e.g., Janches et al., 2000; Pellinen-Wannberg et al., 1998; Sato et al., 2000; Close et al., 2002; Chau and Woodman, 2004). Most of these observations are characterized by the use of very narrow beams (less than 2° half-power full beam widths). The results obtained from these observations have complemented more than 50 years of radar observations with much less-power smaller-antenna specular meteor radars (SMRs) (e.g., Jones and Brown, 1993). For example, Chau et al. (2007) have shown that the sporadic meteor population observed by typical HPLARs is in good agreement with the results obtained from SMRs, in both radiant sources and bimodal velocity distribution. The agreement improves when an altitude threshold is applied to the HPLAR results.

Besides knowing where meteors come from and how HPLAR results compare with SMR results, in recent years significant efforts have been devoted to the study of the meteor mass and sizes and what are the populations observed by the different HPLARs (e.g., Janches et al., 2008; Hunt et al., 2004; Close et al., 2004; Mathews et al., 2001; Bass et al., 2007). Details on the scattering mechanisms that might be behind meteor-head echoes are given by Close et al. (2004). Meteor mass estimates (and sizes) can be obtained from (a) deceleration, and (b) signal-to-noise ratio (SNR). Although there is a general consensus on the physics producing the meteor scattering, good estimates by both measurements required very precise measurements and a reasonable knowledge of the background atmosphere/ionosphere.

In the case of the deceleration method, it is well known now that meteor-head echoes are observed coming from different elevation angles, and not only down the beam. Therefore, measured decelerations are radial and have a component that is due to the geometry and one due to the true deceleration needed for mass estimation. To estimate the former (and later remove it), it is necessary to know the meteor trajectory (e.g., Chau and Woodman, 2004, Eq. (4)).

In the case of the mass estimation using SNR, a precise knowledge of where the meteor is coming from inside the illuminated volume is needed, so that the proper antenna gain is removed before the cross-section is obtained. Such corrections

* Corresponding author.
E-mail address: jchau@jro.igp.gob.pe (J.L. Chau).

1364-6826/$ - see front matter © 2008 Elsevier Ltd. All rights reserved.
doi:10.1016/j.jastp.2008.08.007

could be as large as 20–40 dB. Nowadays, such measurements could be tried at the ALTAIR and Jicamarca radars, where interferometry can be applied. But even then, one has to be very careful in the interpretation, since meteors present a very large dynamic range of cross-sections can be observed with the antenna sidelobes.

In this work, instead of analyzing the results obtained with narrow beams, at the Poker Flat Incoherent Scatter Radar (PFISR) we have implemented a novel wide (W) beam and narrow (N) beam experiment. The main goal of this experiment is to observe meteor-head echoes with large cross-sections that are usually not observed with N beams or are observed in very small quantities. As is well known, larger meteors are expected to occur less frequently, so the probability of observing them with N beams is less than observing them with W beams. Using a W beam will make the interpretation of usual meteor parameters (radial velocity, initial range, radial deceleration, etc.) more complicated than when N beams are used. But as we see below, using the antenna pattern characteristics and the simultaneous W and N measurements, we are able to accomplish our initial goal. Moreover, we are able to identify meteors echoes with large cross-section, previously misinterpreted as small cross-section meteors in N beam observations.

First we present the experimental details and how the wide beam pattern has been implemented using PFISR unique capabilities of changing beam positions from pulse to pulse and allowing phase changes at each antenna element. Basically the W beam is accomplished by defocusing the phase array using a Chirp-like phasing. Then we present the main results obtained with both W and N beams, including the SNR distributions for different groups, depending on which beam the meteor was observed. Finally, qualitative distributions of meteor cross-sections are estimated and discussed using the N SNR as proxy measurement of cross-section.

2. Experiment configuration and antenna compression

PFISR is located at the Poker Flat Research Range near Fairbanks, Alaska (65.13°, 147.47°). PFISR has the unique capability to steer the beam on a pulse-to-pulse basis. The radar is tilted so that its on-axis (or boresight) direction corresponds to elevation and azimuth angles of 74° and 15°, respectively. The beamwidth of PFISR is about $1^\circ \times 1.15^\circ$, with the larger dimension (x) in the plane perpendicular and north to the radar face. Typically, PFISR experiments employ multiple narrow beams almost simultaneously to avoid spatial and temporal ambiguities (e.g., Nicolls et al., 2007; Nicolls and Heinselman, 2007).

The beam positions are obtained by changing the phases of the different antenna element units (AEUS). As it is well known, the antenna pattern of an antenna array is given by the product of the element pattern and the array factor. For small zenith angles, the array factor of the PFISR antenna is given by

$$F_{\text{array}}(\theta_x, \theta_y) = \sum_{i=1}^{M} g_i \exp[jk(x_i\theta_x + y_i\theta_y) + j\phi_i] \quad (1)$$

where $k = 2\pi/\lambda$, M the number of AEUs, x_i and y_i are the positions of the AEUS in meters, θ_x and θ_y are the zenith angles with respect to the on-axis position, and g_i and ϕ_i are the gain and phases (in radians), respectively, for each AEU. Although the PFISR system only allows phase changes, we have included the gain parameter to allow for gaps (i.e., $g_i = 0$ when some AEUs are not used for transmission and/or reception).

As mentioned in the Introduction, instead of sending multiple narrow beams, in this work we have used the unique capabilities of PFISR to transmit a narrow and a wide beam. In typical operations, PFISR transmits a narrow beam by changing the phase linearly with respect to the antenna positions. To transmit (and receive) a wide beam, we have defocused the array by changing the phase quadratically with respect to antenna position, as follows:

$$\phi_i = \phi_{0x} \times (x_i - \bar{x})^2 + \phi_{0y} \times (y_i - \bar{y})^2 \quad (2)$$

where $\phi_{0x} = 0.033$ and $\phi_{0y} = 0.029$ in rad/m^2. Since the antenna array is not square (y larger than x), in order to have a more symmetric beam, ϕ_{0x} is slightly larger than ϕ_{0y}.

This procedure is equivalent to using Chirp (linear frequency modulation) in pulse compression approaches, where wider pulses are transmitted to synthesize narrow pulses with the same average power. A synthetic wide beam approach was used by Woodman and Chau (2001) at the Jicamarca Incoherent Scatter radar, but using complementary binary phase codes in two dimensions. Following the analogy of pulse compression, our approach of transmitting wide beams with a large array is like an antenna compression, since the resulting antenna pattern is equivalent to the pattern of smaller sections of the array, but with the advantage that the total available power is transmitted. If we were to use only a small portion of the PFISR array, the transmitted power would be reduced since PFISR is a distributed transmitted phase array.

In Fig. 1 we show the two-way antenna patterns for a typical narrow beam and different wider beams, all of them pointing on-axis. Fig. 1b shows the theoretical wide beam that one obtains with a quadratic phase change as in Eq. (2) and an amplitude change to avoid the edge effects of a limited array (e.g., using a Hanning-type weighting). The remaining two contour plots show the wide beams using only quadratic phase changes for (c) using all AEUs for transmission and reception, and (d) using the actual AEUs units that were on during transmission and/or reception during the February 2008 experiments. The experiments were conducted on February 20 and 24, 2008 and out of the 4096 AEUs ~97.3% and ~79.5% were on during reception and transmission, respectively. The reason we have fewer transmitting modules is due to failures of a number of solid state power amplifiers (SSPA) and SSPA power supplies. The expected wide beam (Fig. 1c) is indeed wider than the narrow beam, but it has angular structure. Such structure is due to the edge effects, since changes are only done in phase and not in amplitude. The actual wide beam pattern is also wide and very similar to the expected pattern. The differences are due to the malfunctioning AEUs.

To have a closer look at the resulting patterns in Fig. 2 we show selected antenna pattern cuts. At the top normalized patterns are shown in lineal scale, while at the bottom, absolute cuts are shown in relative dB units. The pattern cuts shown are: (a) the narrow beam (N) (in black), (b) the theoretical wide beam using phase and amplitude changes, and (c) the wide beam (W) using only phase changes, for different planes. Usual definitions of antenna beam widths are with respect to the half power points. Since the resulting wide beam pattern presents power changes greater than 3 dB inside its "main" beam, for this work our full beam width is given by the −15 dB points (FBW15). Then the N beam FBW15 is ~1.8°, and for the new W beam FBW15 is ~6.2°.

The main characteristics of these patterns are:

- The maximum gain of N is more than 20 dB larger than the maximum gain of W.
- The sidelobe levels of N are in general similar to the gain of W at the same angles. However, the W beam does not present nulls.

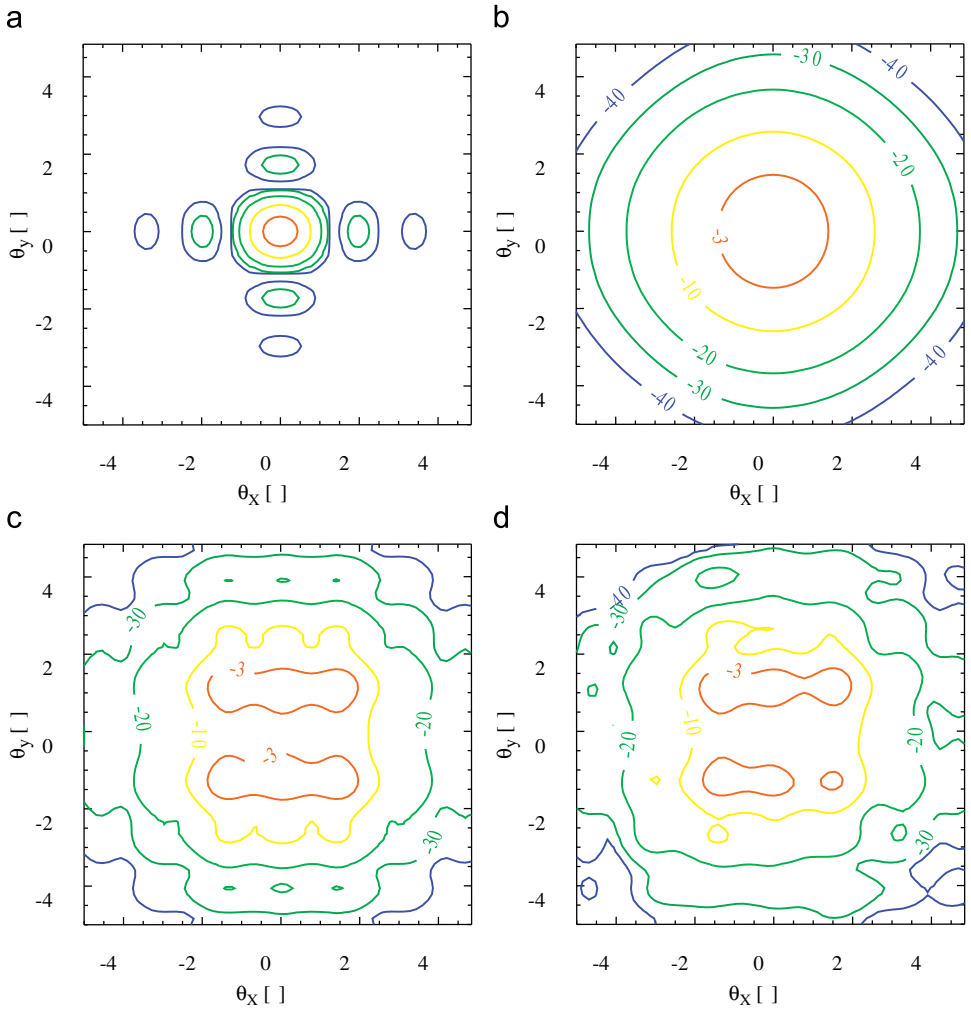

Fig. 1. PFISR antenna patterns as function of θ_x and θ_y angles with respect to its on-axis position. (a) Narrow beam on-axis, (b) wide beam on-axis using amplitude and phase changes, (c) wide beam on-axis using only parabolic phase changes, and (d) same as (c) but taking into account the actual AEUs that were on during transmission and/or reception. The θ_x and θ_y axis are aligned with the x (shorter) and y (larger) sides of the PFISR array. The number in parenthesis represents the antenna code that was programmed.

- The peak of the theoretical wide beam pattern (in blue), would be ~40 dB weaker than the N peak, since a significant fraction of power will not be transmitted due to the amplitude weighting.

The generated W pattern will make the separation of spatial and temporal ambiguities almost impossible for most atmospheric and ionospheric studies. However, as we show in the Results, the main differences of the N and W beams can be used to identify meteor populations that are usually misinterpreted or not detected by typical narrow beam observations.

The experiments presented in this paper were performed on February 20 and 24, 2008 between 12 and 18 UT (LT = UT − 9). The experimental mode consisted of transmitting a N and W beams both pointing on-axis. The beams were sequentially changed from pulse to pulse, i.e., every 2 ms (300 km). Uncoded pulses of 90 μs were transmitted, and samples were obtained from 60 to 290 km every 150 m (i.e., 1 μs). The total transmitted peak power on each beam was about ~1.6 MW.

Within-the-pulse analysis was performed to detect potential meteor-head echoes. The raw data of potential meteor echoes using an SNR threshold of −10 dB, was saved at the site. Later the reduced raw data files were analyzed to characterize the meteor echoes, i.e., to determine their initial range, range and time coverage, radial velocity from a Fourier Transform analysis within the pulse, radial acceleration from the radial velocity time behavior, and the peak SNR. In almost 12 h of observations, 347 and 765 meteor-head echoes were detected and characterized with the W and N beams, respectively.

3. Wide and narrow beam statistics

As shown by Janches and Chau (2005) most of the observed radar parameters (e.g., rates, radial and altitude distributions, etc.) are seasonal dependent. Since our observations are limited to a couple of days in the same season, in this section we concentrate our results and discussions on the similarities and differences of the W and N beam events. More details on narrow beam observations using PFISR can be found in the other meteor papers in this special issue.

In Fig. 3 we present the most relevant statistics of the meteor-head echoes detected with the W (black) and N (red) beams, i.e., (a) time, (b) initial range, (c) range coverage, (d) time coverage, (e) radial velocity, and (f) radial acceleration. With the W beam we

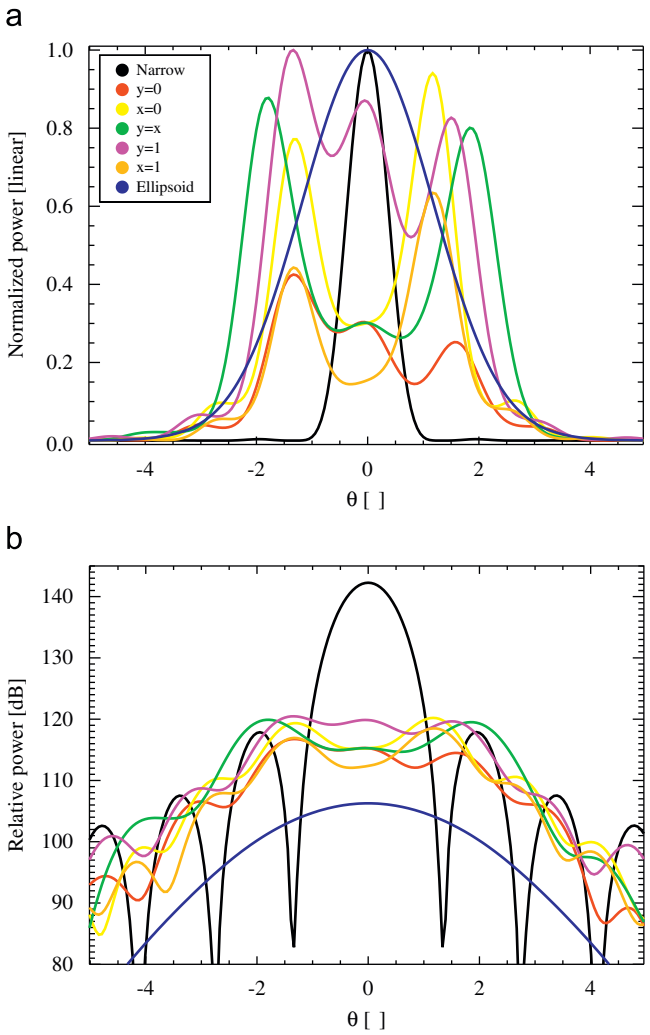

Fig. 2. Antenna pattern cuts for the N beam (in black). The different color lines represent different cuts for the implemented W beam, except for the blue line that represents a theoretical beam obtained changing the phase and amplitude. (a) Normalized patterns in lineal scale, and (b) relative power patterns in dB scale.

are observing ~54.6% less meteors than with the N beam. The main findings from these statistics are:

- Most of the results are consistent with meteors coming "around" the main N beam (i.e., within the FBW15). For example, most meteors in the W have similar altitudinal distribution as in N, but with less events.
- However, there is a significant population of meteors indicating that they are either coming from very low elevation angles (sidelobes in N) or with low elevation trajectories. For example, meteors with initial range greater than 120 are observed with same statistics in both the N and W beams. Similarly the low radial velocity ($<5\,km/s$) and the radial decelerations ($\geqslant 0\,km/s^2$), are consistent with this finding.
- The range and time coverage histograms are shown normalized to their respective peaks. In these normalized plots we can clearly see that proportionally speaking the W beam meteor echoes are observed for a longer time and range.

As shown by Chau and Woodman (2004) without interferometry capabilities, it is difficult to interpret meteor-head echo results, since meteoroids could come with different elevation angles. Even if very narrow beams are used, given the meteor echo large dynamic range of cross-sections, they can be observed at different zenith angles, as shown in the above results. Note that the observations were taken near the Spring Equinox when the Apex never rises much above the horizon at the latitude of PFISR. Given that the Apex source dominates the sporadic meteor population (e.g., Chau et al., 2007), besides changes in the radial velocity and acceleration distributions, significant changes are expected in the number of detected echoes at different seasons (e.g., Janches et al., 2006).

Can we identify from N beam observations how many events are coming from sidelobes? How many are actually coming from the mainlobe?

4. SNR and meteor-head cross-section

Fig. 4 presents examples of SNR vs. time for meteor-head detections with both W (black) and N (red) beams. The left figure is an example of a meteor echo that has been observed with the N mainlobe. Note that the difference in peak SNR is more than 20 dB as expected from the calculated beam patterns (e.g., Fig. 2b). The right figure shows an example of a meteor echo that has been observed with an N sidelobe, since the SNR values are similar to the W beam results.

Although not the main purpose of this paper, given the excellent agreement between the theoretical antenna pattern with the SNR profile of Fig. 4a, the SNR time profiles of narrow beams could be used to determine the meteor trajectory. For example, if multiple narrow beams around the on-axis beam are used, meteor trajectories can be found for some meteor events, particularly those coming at low elevation angles and last long enough as to be observed by more than one of the main narrow beams. Using the Jicamarca HPLA radar, Chau et al. (2008) have recently used the SNR time profiles of meteor-head echoes, not to detect their trajectory, but to calibrate the system phases of interferometric configurations. Briefly, the procedure consists of finding the system phases that maximizes the agreement between the meteor echo SNR and the expected antenna pattern cut. The cross-section of the meteor echo could change, but as long as the change is small compared to the changes due to the antenna pattern, the phase calibration procedure works.

Using the time and range information of meteor echoes of both beams, in Fig. 5 we show the SNR distribution of (a) all the detected events, (b) events detected simultaneously by the W and N beams (i.e., with similar time and range), and (c) events detected in only one beam. From Fig. 4 and the antenna pattern characteristics described in the previous section, we can conclude that (a) the events observed only with the N beam are coming from the N mainlobe (note that these events present SNR less than 15 dB), and (b) the events observed only with the W beam are coming outside the N mainlobe, therefore they are at least 20 dB stronger if they were observed with the N mainlobe. Can we tell more about the meteors observed simultaneously by the W and N beams? The answer is yes. Using the SNR difference between the W and N simultaneous events, we can identify those meteors that were observed outside the typical 3–10 dB beam width.

In Table 1 we summarize the results of the different populations that we can identify using the W and N beam observations along with the SNR and antenna pattern characteristics. The first four rows indicate very simple statistics. By considering that our empirical detectability level is close to −5 dB SNR, then meteor-head echoes with SNR greater than15 dB in N would be observable by the W beam, i.e., at least 62 of the N beam would be observable by the W beam. However, we observed 159 meteor heads in both W and N beams. Since a meteor observed in the W beam is at least 20 dB stronger if they

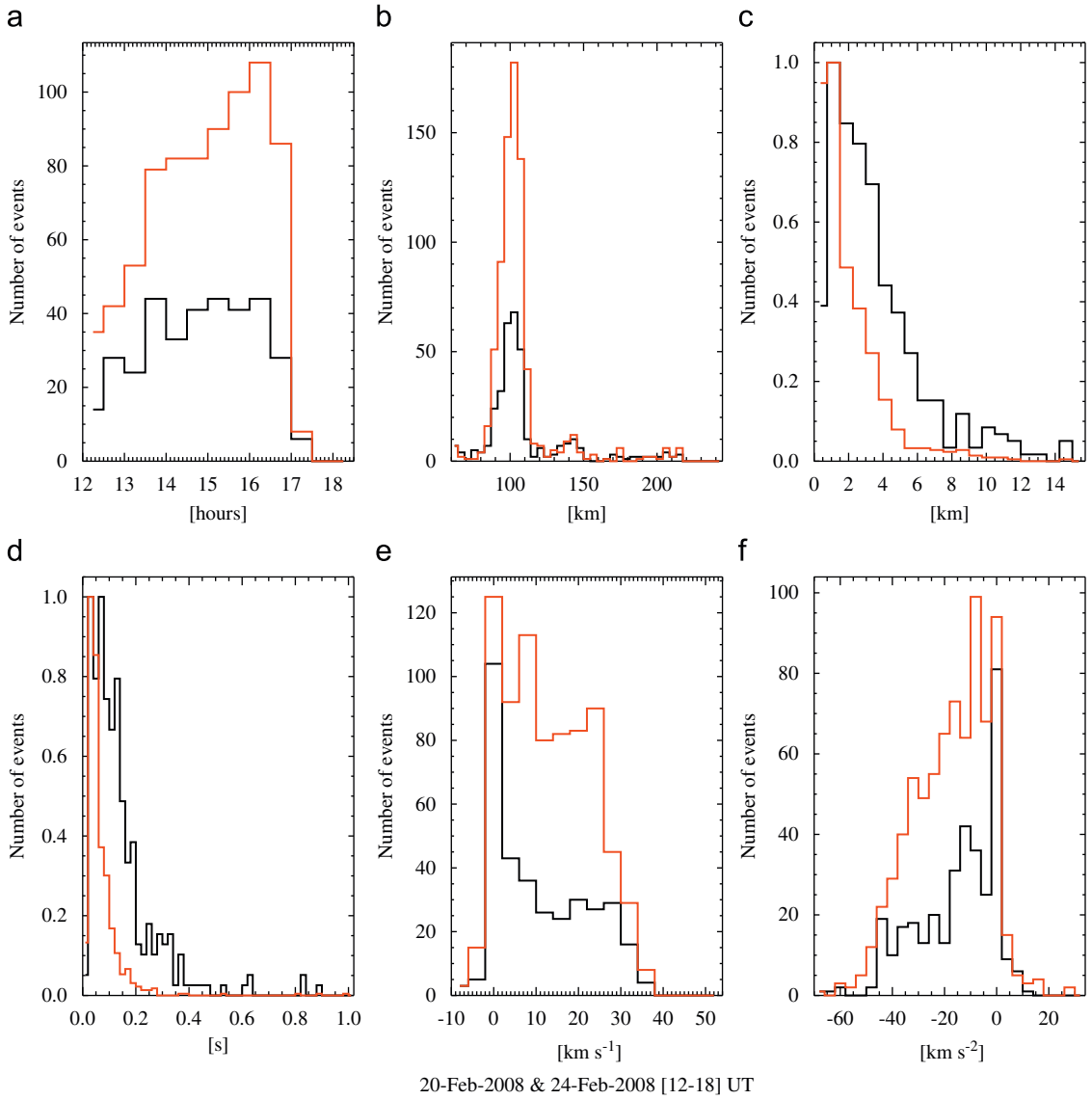

Fig. 3. Selected meteor-head statistics from observations performed between 12 and 18 UT (LT = UT − 9) on February 20 and 24, 2008 with PFISR. The wide beam results are shown in black, while the narrow beam in red for: (a) universal time, (b) initial range, (c) range coverage, (d) time coverage, (e) radial velocity, and (f) radial acceleration. Note that the range and time coverage statistics have been normalized.

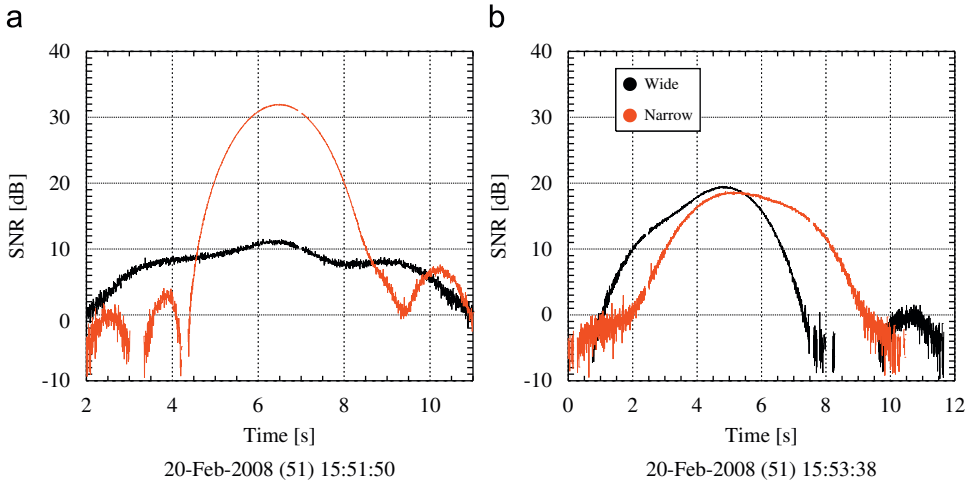

Fig. 4. Examples of SNR vs. time for meteor-head echoes observed in both the W (black) and N (red). (a) An event observed in the N mainlobe, and (b) an event observed in one of the N sidelobes. Note that the difference in peak SNR is more than 20 dB when a meteor-head is observed in the mainlobe.

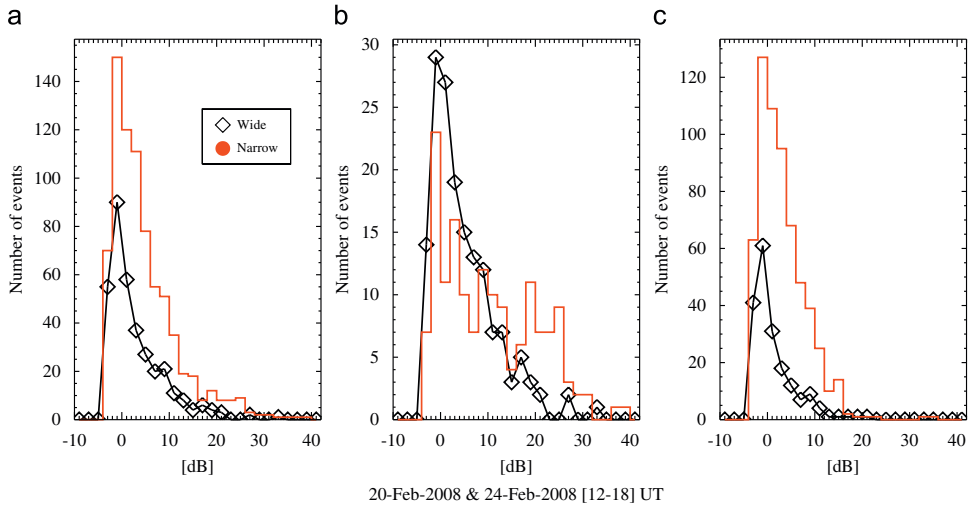

Fig. 5. SNR statistics for different meteor-head populations based on concurrent W and N beam observations. (a) All events for W (black, ⋄) and N (red) beams, (b) events observed simultaneously with the W and N beams, and (c) events observed only in one beam, either W or N.

Table 1
Selected meteor-head statistics based on SNR measurements with wide (W) and narrow (N) beams

SNR meteor-head statistics			
Description	Criteria	N equivalent	Count
All N	All N	+0 dB	765
All W	All W	+0 dB	347
All "big" N	All N, $SNR_N > 15$ dB	+0 dB	62
N and W	N = W	+0 dB	159
Only N	Only N	+0 dB	606
N = W in N sidelobe	N = W, $SNR_N - SNR_W < 15$ dB	+20 dB	117
N = W in N mainlobe	N = W, $SNR_N - SNR_W \geqslant 15$ dB	+0 dB	37
Only W	Only W	+20 dB	188

were observed by the N mainlobe, we are indeed detecting more "stronger" meteors with the W beam.

In the second part (rows 5–8), we present the statistics of meteor echoes as if they were observed with the N mainlobe. Moreover, using the SNR as proxy measurement of effective meteor cross-section (e.g., Close et al., 2004), in the third column we indicate a conservative correcting number that should be added to the measured SNR to get a proxy meteor cross-section in N relative units. The fifth row ("Only N") shows the meteors observed by the N mainlobe, so there is no correction needed. The sixth row (N in sidelobe) indicate that 117 out of 765 (i.e., ~15%) N meteor-heads are coming outside the mainlobe, and their relative N cross-section is at least 20 dB stronger. The seventh row (N in mainlobe) shows that only 37 meteor-heads are coming from the N mainlobe. For the last two groups we have used the difference between the N and W SNR ($SRN_N - SNR_W$) as a selector criterium. Finally, in the eighth row we show the events that were observed only with the W beam (188). Since the W beam is at least 20 dB weaker than the N mainlobe peak, the W SNR needs to be corrected at least 20 dB to be in N relative cross-section units.

To simplify the results in Table 1, in Fig. 6 we present a proxy measurement of cross-section using the N SNR. In Fig. 6a, the red histogram represents the histogram of all N events. If we assumed that all the meteors come from the typical mainlobe (3–10 dB weaker than the peak), then this distribution (with 3–10 dB difference) represents the true cross-section distribution in N relative units. But using the information in Table 1, the corrected distribution of all the N event is given by the black (△) cumulative distribution that has been obtained by combining the different sub groups: only N, N events in sidelobe (N = W), and N events in mainlobe (N = W). Green (⋄) events represent the "only N" plus "N = W in N sidelobes", therefore green (⋄) minus blue represent the "large" meteor cross-sections that have been detected outside the N mainlobe. The black (△) minus the green (⋄) events are the strong meteors detected inside the mainlobe. We can observe a clear redistribution of meteors. Using the W beam information, we are able to identify more large cross-section events, the resultant distribution should be closer to the true histogram distribution of meteor cross-section using a narrow beam. The sudden change around 15 dB is due to: (a) the correcting numbers are approximate conservative numbers, and (b) there is a population of meteor echoes below 15 dB that its actual value could be 3–10 dB larger and without interferometry it is impossible to make the correction.

Fig. 6b shows similar information, but for the combined N and W events. In this case we are adding the events that were observed only by the W beam. These events represent mainly those detected by the W beam where there are antenna nulls in the N beam pattern, again, we have used a 20 dB correction to have them in N relative cross-section units. The red histogram represents all the N events as a reference. The distribution of the original N plus only W events are shown in blue, while the distribution of the corrected N plus only W is shown in black (□). Besides helping identify large cross-section events in N beam data, the W results have allowed to detect close to 10 times more large cross-section events. It is important to mention that the black distribution does not represent the true distribution of cross-section (SNR) vs. number of events, it represents an approximate distribution of cross-section vs. number of events that can be obtained combining the W and N beam. The sudden peak around 20 dB is due to the lack of sensitivity of the W beam to detect meteor echoes with cross-sections lower than that number.

5. Discussion and concluding remarks

As mentioned in the Introduction, the main objective of our W beam experiment (FBW15~6.2°), was to observe more meteor events with larger cross-section than those observed with typical N (FBW15~1.8°) beams. Based on the results summarized in Table 1 and Fig. 6, we have accomplished such goal, by detecting 347

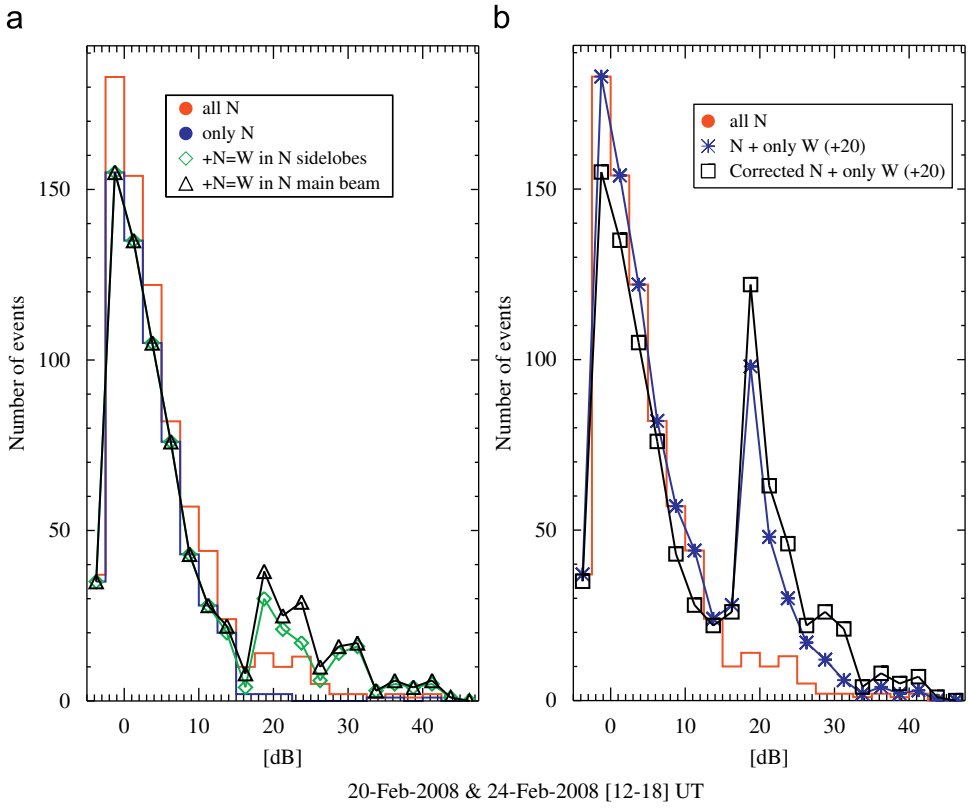

Fig. 6. Qualitative proxy measurements of meteor-head cross-section based on SNR measurements using the main N beam as a reference. In panel (a) the distribution of all N meteors is represented in red, while the distributions of other N subgroups with different colors and symbols. The black distribution (△) represents the corrected cross-section distributions of all N events (see main text for a description of the other two subgroups). In panel (b) we show the combined distributions of W and N beams: all N plus only W after 20 dB correction (blue, ∗), and the corrected N plus only W after 20 dB correction (black, □). As a reference we have included the distribution of all N (red).

meteor events that if they were detected by the N beam, they would have been observed at least 20 dB stronger. This number is ∼10 times more the strong echoes detected in the N mainlobe (37). Note that 20 dB is a very conservative number, since a more aggressive correction could be 20–40 dB.

In addition, by combining the W and N beams, we have been able to determine that at least 15% of the events detected with the N beam were coming from outside the mainlobe, i.e., they are at least 20 dB stronger if they were to be observed by the N mainlobe. Moreover, for the majority of N beams detected inside the mainlobe its actual cross-section could vary between 3 and 10 dB. These results indicate that a significant fraction of meteors are coming from outside the mainlobe, therefore mass estimates using SNR at PFISR or any other HPLA radar (e.g., Janches et al., 2008; Close et al., 2004) should be interpreted with caution. Meteor-head echoes present a large dynamic range of cross-sections therefore it is very difficult, if not impossible, to determine where in the sky (not just the mainlobe region) the echo is coming from. To try to get around this limitation, an interferometry configuration with at least three non-collinear antennas is needed.

Based on our experience at Jicamarca (e.g., Chau and Woodman, 2004; Chau et al., 2007), this task could require more than three antennas to combine long baselines for precision and sensitivity with short baselines to remove the angular ambiguity. Interferometry not only would help on the determination of mass using SNR but also in the determination of mass using deceleration values (e.g., Mathews et al., 2001; Close et al., 2004; Bass et al., 2007). As pointed out by Chau and Woodman (2004), the measured deceleration is a mixed of geometry contributions (a non decelerating meteor coming off-zenith will present a radial deceleration) and actual deceleration. To remove the former it is necessary to know the meteor trajectory (i.e., azimuth and elevation) parameters that can be obtained with interferometry.

Having shown that with W beams we are able to observe more meteors with larger cross-section, in the future we plan to study the characteristics of these larger cross-section population. For example, compared to the majority of smaller cross-section events, do they present the same absolute velocity and altitude distribution? Do they come from the same region in the sky? With the current dataset we could get some statistics (radial velocities, initial ranges, etc.) but since they are radial quantities, we do not think the results will be representative. While interferometry is being implemented at PFISR, we plan to conduct a new W and N beam experiment but this time at Jicamarca using interferometry and an binary phase antenna compression scheme (Woodman and Chau, 2001).

Finally, we plan to run the W and N beam configuration at PFISR during strong meteor shower events, like the Quadrantids, one of the strongest annual showers with a high northern declination (49°). Although meteor shower events can be detected by HPLA radars (Chau and Galindo, 2008), they are difficult to detect and identify with single narrow beam radars. Since meteor shower events are expected to have larger cross-sections but with less frequency of occurrence than sporadic meteors (e.g., Jenniskens, 2006), by increasing the observing volume we might be able to separate the shower events from the typical sporadic distributions.

Acknowledgments

The data collection and analysis for PFISR was supported under NSF cooperative agreement ATM-0608577. J.L.C. and F.R.G. were supported under NSF cooperative agreement ATM-0432565.

References

Bass, E., Chau, J.L., Oppenheim, M., Olmstead, A., 2007. Improving the accuracy of meteoroid mass estimates from head echo deceleration. Earth, Moon and Planets, doi:10.1007/s11038-0079202-2.

Chau, J.L., Galindo, F., 2008. First definitive observations of meteor shower particles using a high-power large-aperture radar. Icarus 194, 23–29.

Chau, J.L., Woodman, R.F., 2004. Observations of meteor-head echoes using the Jicamarca 50 MHz radar in interferometer mode. Atmospheric Chemistry and Physics 4, 511–521.

Chau, J.L., Woodman, R.F., Galindo, F., 2007. Sporadic meteor sources as observed by the Jicamarca high-power VHF radar. Icarus 188, 162–174.

Chau, J.L., Hysell, D.L., Kuyeng, K.M., Galindo, F.R., 2008. Phase calibration approaches for radar interferometry and imaging configurations: equatorial spread F results. Journal of Atmospheric and Solar-Terrestrial Physics, this issue, doi:10.1016/j.jastp.2008.08.007.

Close, S., Oppenheim, M., Hunt, S., Dyrud, L., 2002. Scattering characteristics of high-resolution meteor head echoes detected at multiple frequencies. Journal of Geophysical Research 107.

Close, S., Oppenheim, M., Hunt, S., Coster, A., 2004. A technique for calculating meteor plasma density and meteoroid mass from radar head echo scattering. Icarus 168, 43–52.

Hunt, S., Oppenheim, M.M., Close, S., Brown, P., McKeen, F., Minardi, M., 2004. Determination of the meteoroid velocity distribution at the Earth using high-gain radar. Icarus 168, 34–42.

Janches, D., Chau, J.L., 2005. Observed diurnal and seasonal behavior of the micrometeor flux using the Arecibo and Jicamarca radars. Journal of Atmospheric and Solar-Terrestrial Physics 67, 1196–1210.

Janches, D., Mathews, J.D., Meisel, D.D., Zhou, Q.H., 2000. Micrometeor observations using the Arecibo 430 MHz radar I. Determination of ballistic parameter from measured Doppler velocity and deceleration results. Icarus 145.

Janches, D., Heinselman, C.J., Chau, J.L., Chandran, A., Woodman, R.F., 2006. Modeling the global micrometeor input function in the upper atmosphere observed by high power and large aperture radars. Journal of Geophysical Research 111.

Janches, D., Close, S., Fentzke, J.T., 2008. A comparison of detection sensitivity between ALTAIR and Arecibo meteor observations: can high power and large aperture radars detect low velocity meteor head-echoes. Icarus 193, 105–111.

Jenniskens, P., 2006. Meteor Showers and Their Parent Comets. Cambridge University Press, UK.

Jones, J., Brown, P.G., 1993. Sporadic meteor radiant distribution: orbital survey results. Monthly Notices of the Royal Astronomical Society 265, 524–532.

Mathews, J.D., Janches, D., Meisel, D.D., Zhou, Q.H., 2001. The micro-meteoroid mass flux into the upper atmosphere: arecibo results and a comparison with prior estimates. Geophysical Research Letters 28, 1929–1932.

Nicolls, M.J., Heinselman, C.J., 2007. Three-dimensional measurements of traveling ionospheric disturbances with the Poker Flat incoherent scatter radar. Geophysical Research Letters 34.

Nicolls, M.J., Heinselman, C.J., Hope, E.A., Ranjan, S., Kelley, M.C., Kelly, J.D., 2007. Imaging of polar mesosphere summer echoes with the 450 MHz Poker Flat advanced modular incoherent scatter radar. Geophysical Research Letters 34.

Pellinen-Wannberg, A., Westman, A., Wannberg, G., Kaila, K., 1998. Meteor fluxes and visual magnitudes from EISCAT radar event rates: a comparison with cross-section based magnitudes estimates and optical data. Annales de Geophysique 116, 1475–1485.

Sato, T., Nakamura, T., Nishimura, K., 2000. Orbit determination of meteors using the MU radar. IEICE Transactions on Communications E83-B, 1990–1995.

Woodman, R.F., Chau, J.L., 2001. Antenna compression using binary phase coding. Radio Science 36, 45–52.